Analysis vs Centrifuge Seismic Experiments for U-shaped Cantilever Retaining Walls

L. Tsantilas, E. Garini, and G. Gazetas
Soil Mechanics Laboratory, National Technical University, Athens, Greece

ABSTRACT
A numerical analysis of the seismic response of a U-shaped non-displacing cantilever wall in a two-layered sand stratum is performed, properly modeling the wall-soil interface, to allow separation and sliding. The results are compared with the centrifuge results of Mikola and Sitar (2013). A parametric numerical study gives further insight in the dynamics of the system.

Both the test and our analyses employ several near-fault ground motions recorded in Kocaeli 1999, Kobe 1995 and Loma Prieta 1989, such as Yarimca, Takatori, Santa Cruz, and Saratoga West Valley College. Results are presented in terms of acceleration time histories, acceleration, velocity and displacement spectra, dimensionless wall moment distributions, and dynamic soil pressures. Comparison with the Mononobe-Okabe method is performed as well, and practically significant conclusions are drawn.

1 INTRODUCTION: CANTILEVER RETAINING WALLS

In state-of-practice, a cantilever retaining wall is formed by a vertical part connected to a slab foundation, while its stability mechanism is based on the action of the backfill soil. A special type of cantilever walls is the U-shaped, which restrain the retained earth by the passive resistance provided by the opposite wall. The major advantage of cantilever walls is their simple construction. However, they are not recommended to use next to adjacent buildings if strict horizontal displacement limits exist. Control of lateral wall displacement is the major design objective. The magnitude of horizontal wall deflections depends on the passive earth resistance mobilization.

Cantilever walls, in practice, are designed with limit equilibrium methods. The Mononobe-Okabe method (1926), an extension of Coulomb's method, is the earliest and most widely used analytical method. It gives the total active thrust acting on the wall by applying a pseudostatic inertial force on the soil wedge. Despite its known drawbacks, the classic pseudo-static Mononobe–Okabe (M–O) formula is still the main method proposed for the analysis of yielding walls. Since then, numerous analytical, experimental, and numerical studies have been published for the dynamic behavior of retaining walls. The M–O method had been modified and simplified by Seed & Whitman (1970). Richards & Elms (1979) determined permanent (inelastic) outward displacements, and Nadim & Whitman (1983) permanent sliding and rotation using the Newmark sliding block concept. Veletsos and Younan (1994) modelled the soil as an elastic medium and obtained elastodynamic solutions. Several other studies have also appeared, among which [2], [27], [12], [5] [10], [13], [22] and [6]. In parallel, a significant effort was made in numerical study of seismic earth pressures in centrifuge experiments, as referred, by [21], [4], [28], [25], [18)], [14], [1], and most recently by Mikola & Sitar (2013).

The scope of this paper is to shed more light into fundamental aspects of seismic response of cantilever retaining walls subjected to near-fault ground shaking, by numerical verification of the centrifuge experiments of Mikola and Sitar (2013); experiments which will be presented in the following section.

The aforementioned scope is in accordance with the foundations of performance-based design, in order to upgrade significantly the traditional methods of seismic design and shed light on the complete soil-foundation-structure system.

Figure 1. The large centrifuge payload bucket at the Center for Geotechnical Modeling at U.C. Davis.

2 THE CENTRIFUGE EXPERIMENT

Two centrifuge experiments were performed by Mikola

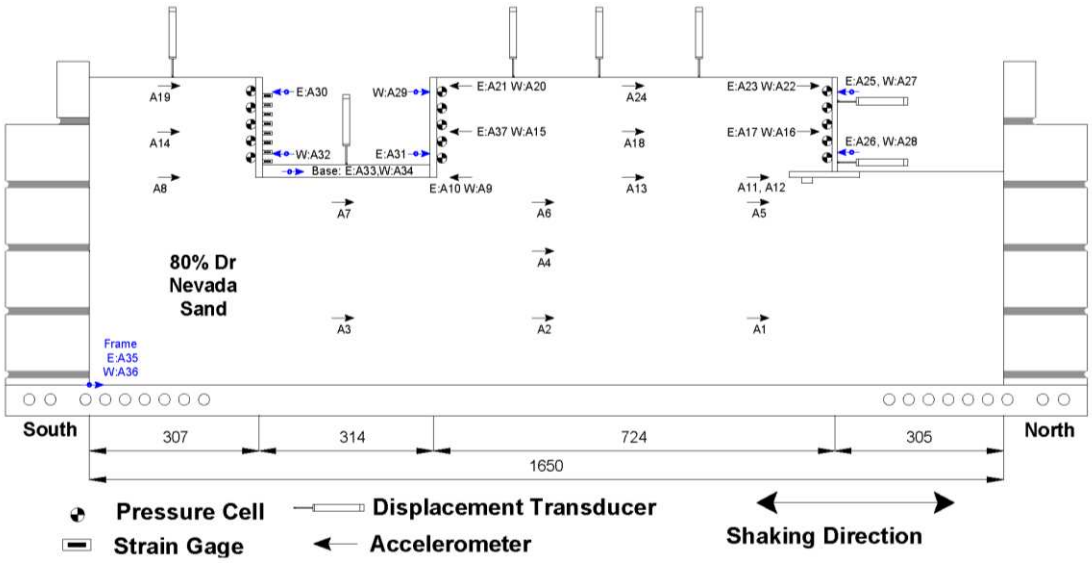

Figure 2. ROOZ02 Model configuration, profile view (dimensions in mm, from Mikola, G.R. and Sitar, N. 2013)

and Sitar (2013) on the dynamic centrifuge at the Center for Geotechnical Modeling at the University of California, Davis. The centrifuge has a radius of 9.1 m, and an available bucket area of 4 m^2 as pictured in Figure 1.

The shaking table can operate up to a maximum centrifugal acceleration of 75 g. For the particular experiments, the centrifugal acceleration used in was 36 g. The first centrifuge experiment, named ROOZ01, was performed on uniform dense sand, whereas the second centrifuge experiment, ROOZ02, on a two-layer sand model.

In a previous study, the results of the displacing cantilever wall of the second experiment were verified numerically (Garini et al. 2016). In this study, it is interesting to verify numerically the results of the non-displacing U-shaped cantilever wall of the second experiment, as depicted in Figure 2.

The ROOZ02 model consisted of a non-displacing U-shaped cantilever and a displacing inverted T-shaped retaining wall. The structures were founded on approximately 12.5 m of dry dense sand (Dr = 80%) and support a dry medium-dense sand backfill (Dr = 75%) as can be seen in Figure 3.

The model soil was dry Nevada Sand. Retaining structures were constructed of T6061 aluminum plate. The non-displacing U-shaped cantilever wall was constructed by three plates: two parallel plates which were bolted to a base plate. Geometry and dimensions of this cantilever structure in prototype scale is pictured in Figure 3. Ten shaking events were applied to the ROOZ02 model in flight. The excitations examined herein, are: the Yarmica recorded ground motion during the 1999 Kocaeli earthquake, the Santa Cruz shaking by the 1989 Loma Prieta event, and the Takatori ground motion of the 1995 Kobe earthquake.

Six types of electronic transducers were employed for measuring in the experiment: accelerometers, strain gages, pressure transducers, linear potentiometers, variable differential transformer, and load cells. With these devices were evaluated the acceleration on the retaining wall and backfill soil, the bending strains and deflections, the backfill settlements, and the lateral earth pressures acting on the cantilever wall.

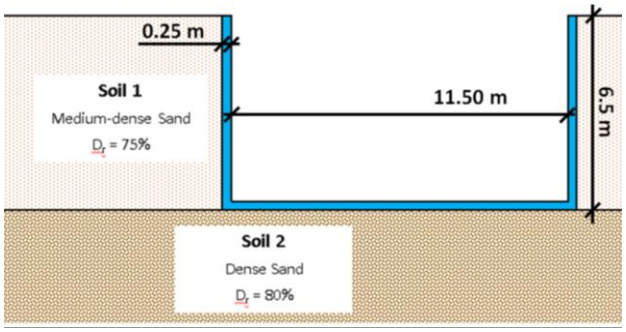

Figure 3. Sketch of U – shaped cantilever wall verified in this study, showing the foundation and backfill soil characteristics, and the dimensions in prototype scale.

3 VERIFICATION: FINITE ELEMENT MODEL AND MATERIALS

A 2-D plane-strain finite element model was constructed using the ABAQUS finite element commercial code. The discretization consists of four noded quadrilateral, plane-strain elements as shown in Figure 4. Interface between wall and soil appropriately modeled as tensionless but frictional; it is simulated with special elements that allow separation and sliding, the latter controlled by coefficients of friction μ. To capture radiation damping, normal and shear viscous elements ρV_S and ρV_P (per unit area) are placed at the vertical boundaries between the soil domain and the vertical free-field columns, which are introduced on each side in order to have proper transmission of up-coming waves thus, avoiding the box effect.

The geometrical limits of the model are 11 m behind each wall plate. This dimension was selected after various sensitivity runs performed to determine the effect of the boundaries on the results. The soil properties are: (i) for the retained soil: ρ_1 = 1.695 Mgr/m^3, E_1 = 450 MPa, φ_1 = 35°, ψ_1 = 5° and c_1 = 2 kPa; (ii) for the foundation soil: ρ_2 = 1.695 Mgr/m^3, E_2 = 675 MPa, φ_2 = 42.5°, ψ_2 = 12.5° and c_2 = 3 kPa. Some of the soil properties are taken equal to the initial input parameters for the UBCHYST soil properties in the numerical model of Mikola & Sitar (2013), and the rest of them are properly calibrated to simulate the physical properties of such soils. The wall is made from concrete and its behavior presumed to be elastic. The coefficient of friction is μ = 0.34 between the retaining wall and the foundation and backfill soil.

Soil behavior is described by a refined soil model developed by Gerolymos et al (2006) and Anastasopoulos et al (2011), utilized through a subroutine attached to ABAQUS. It models the nonlinear soil inelasticity through a simple kinematic hardening with Von Mises failure criterion and an associative flow rule. The evolution law consists of two components: a nonlinear kinematic hardening component describing the translation of the yield surface in stress space, and an isotropic hardening component, which defines the size of the yield surface as a function of plastic deformation.

For the purposes of the present study, model parameters were systematically calibrated, according to the G-γ and ξ-γ curves curves employed by Mikola & Sitar (2013). A value of model's parameter, λ, was found to provide a reasonable fit to G-γ curves. The computed τ-γ (shear stress-shear strain) hysteresis loops (because of the adoption of the Masing criterion for loading-unloading) result in overestimating the hysteretic damping for large shear strain amplitudes ($\gamma \approx 10^{-2}$). Details for the validation of the model can be found in the afore-cited references.

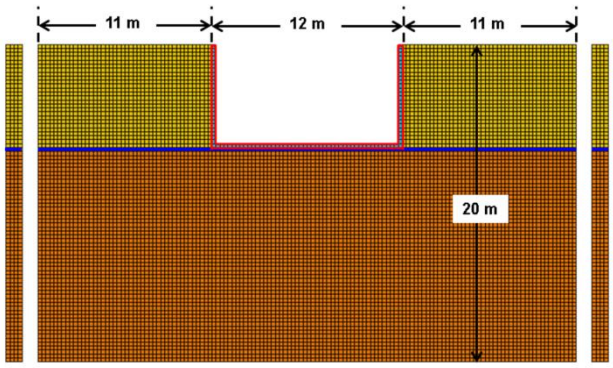

Figure 4. The ABAQUS finite element model configuration.

4 VERIFICATION: RESULTS

The verification is performed in terms of acceleration time histories (and their corresponding acceleration, velocity and displacement elastic spectra), maximum bending moments of the wall, and soil pressure distribution along the depth of the left wall. All results are presented in terms of prototype units and they refer to two characteristic points shown in Figure 5. The nomenclature of these points is the same with the one in the report of Mikola & Sitar (2013).

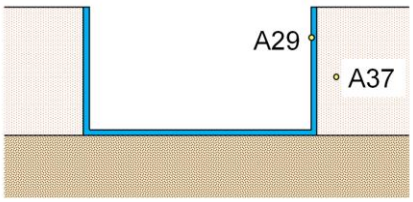

Figure 5. Geometry of the two characteristic points where our analysis results are focused.

For the sake of brevity, only a minimum of all the parametric results are presented below. Figure 6 illustrates the acceleration time histories and their corresponding acceleration, velocity and displacement elastic spectra in points A29, A37 induced by the Santa Cruz excitation. The black solid line corresponds to centrifuge and the red solid line to our numerical analysis. The very good agreement between the experiment and the analytical response is evident. Not only the maxima are captured but also the smaller details of the motion. Also, the frequency content of the accelerograms is reproduced as well. The agreement of the frequency-amplitude is portrayed better in terms of the response spectra of Figure 6. Either at the wall point (A29) or the backfill soil (A37), numerical response is very close to the experimental one, and this is true not only for the Santa Cruz excitation but for Yarimca too, as it is depicted in Figure 7.

So, in the micro scale of soil - structure point agreement is achieved, but is this valid in the macroscopic level of the whole system? To answer this question, the distribution of maximum bending moments of the left stem from the centrifuge experiment is compared with the numerical response. To this end, Figure 8 depicts the comparison of the dimensionless wall bending moment, $M/\gamma H^3$, with depth over wall's height, z/H, for all three studied ground motions. The centrifuge data are plotted with the yellow diamond shaped line and the F.E. results with the red solid line. In all cases, the comparison between the experiment and the numerical analyses is satisfactory. No large diversions are observed and the trends are quite the same.

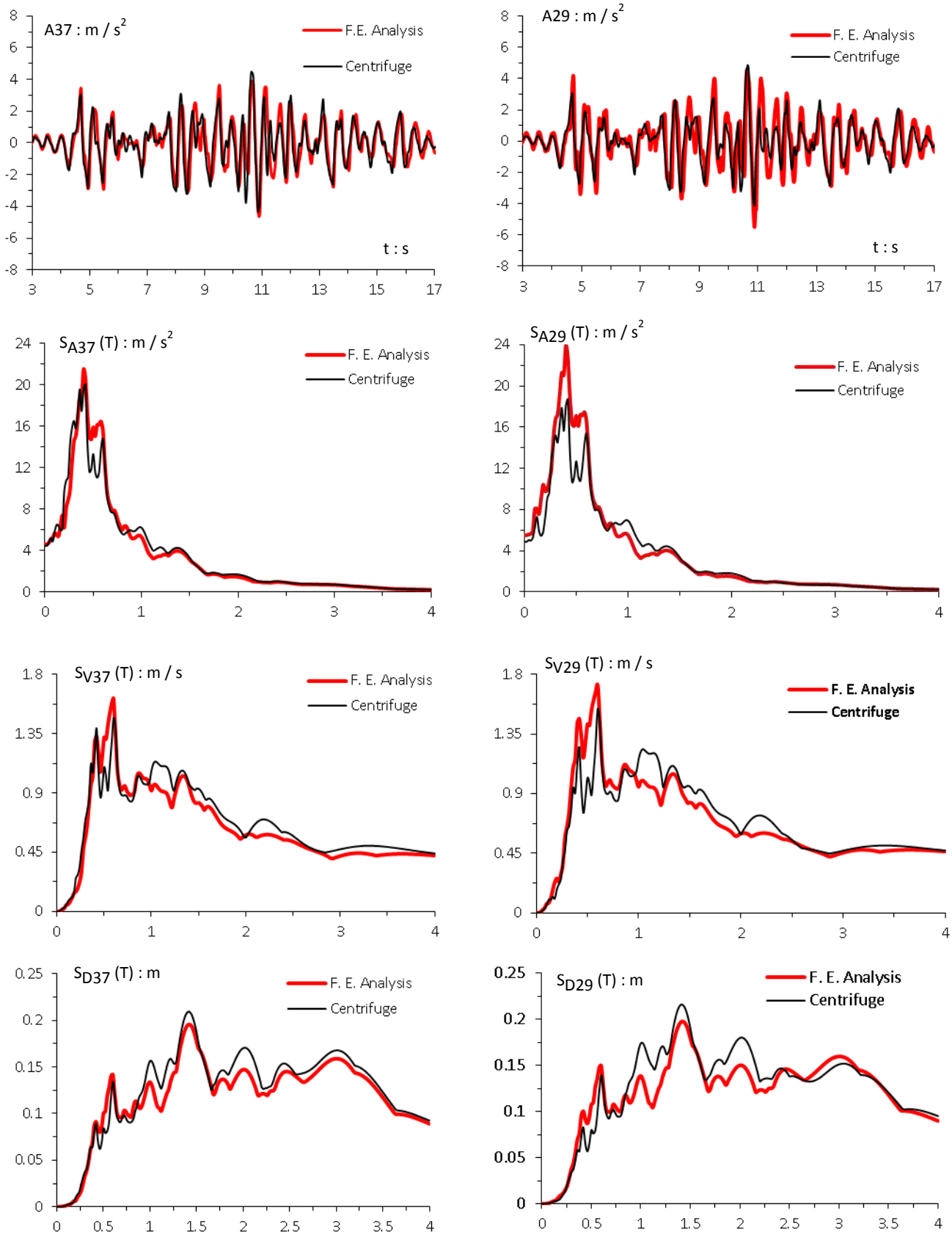

Figure 6. Comparison of acceleration time histories, their respective acceleration, velocity and displacement spectra, at two characteristic points [Point A37 left, Point A29 right, Excitation: Santa Cruz].

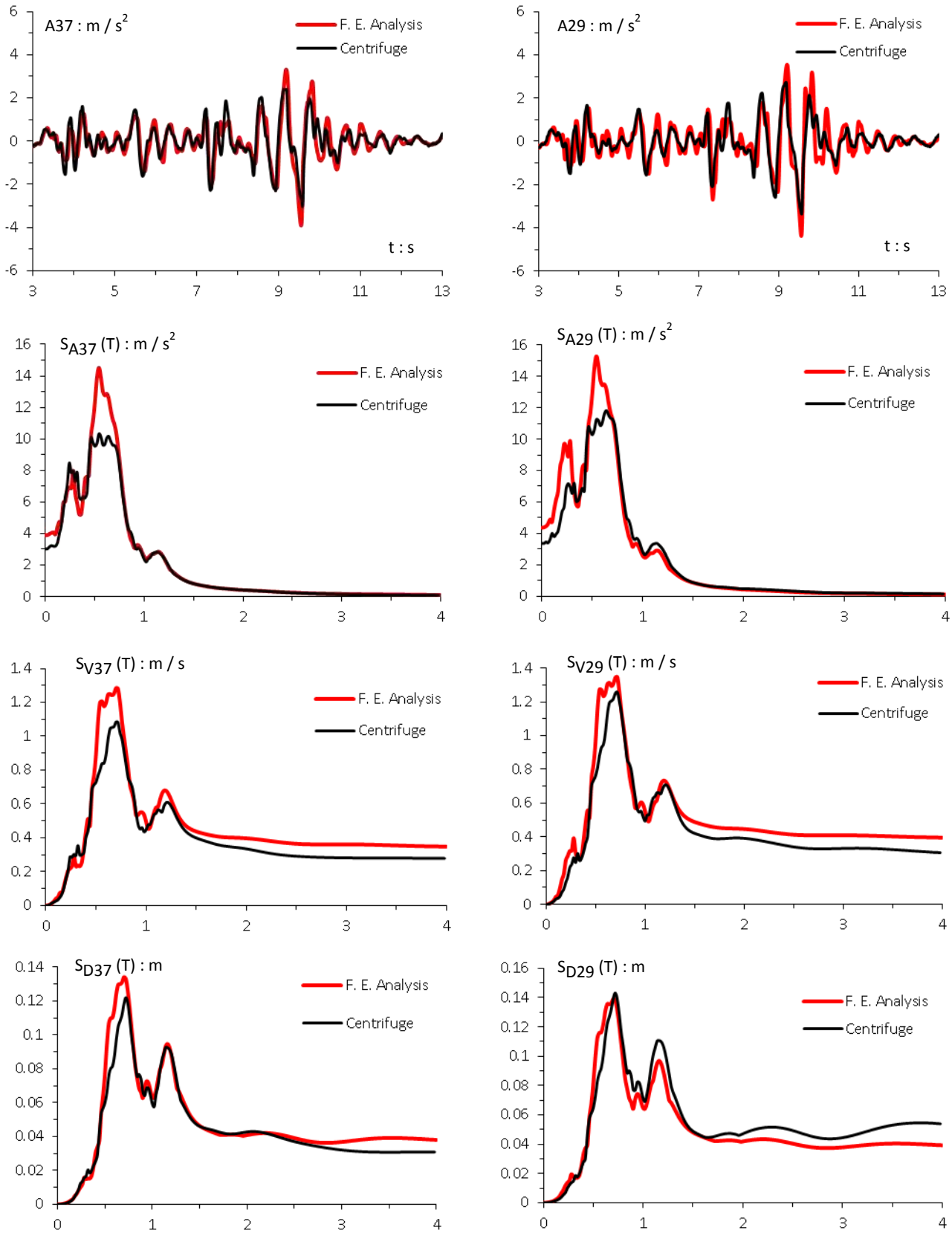

Figure 7. Comparison of acceleration time histories, their respective acceleration, velocity and displacement elastic spectra, at two characteristic points [Point A37 left, Point A29 right, Excitation: Yarimca].

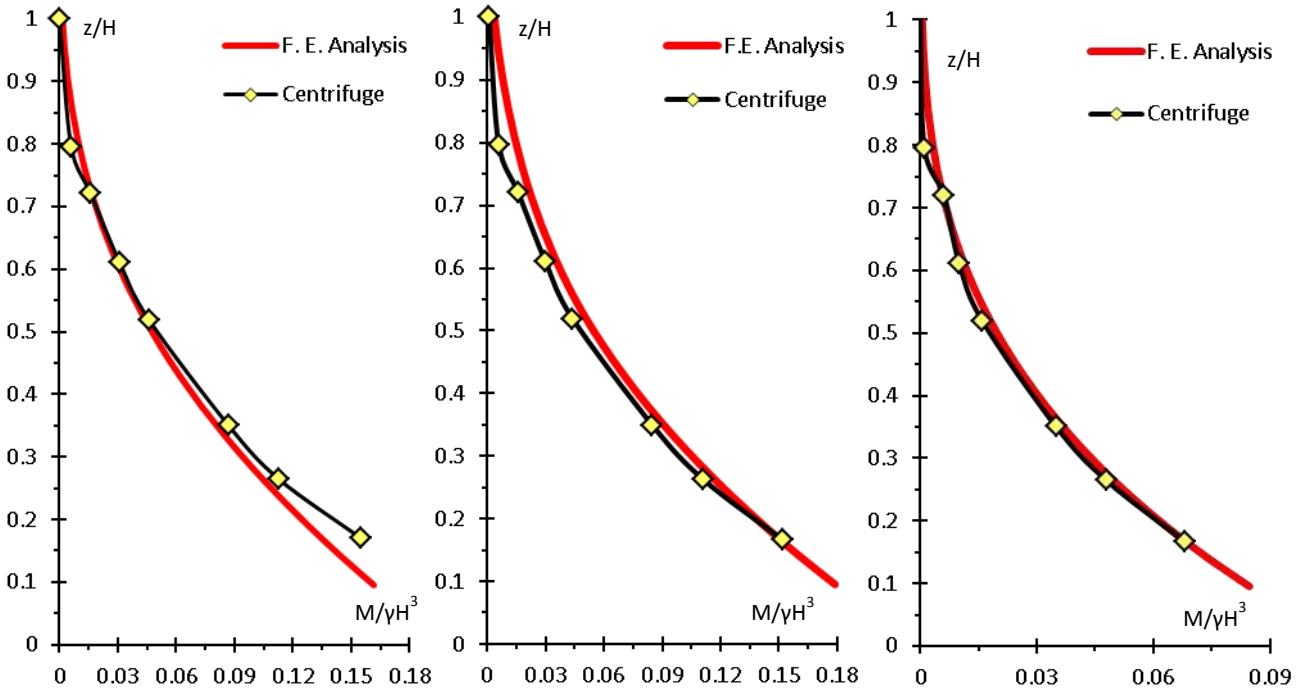

Figure 8. Comparison of dimensionless bending moment of the wall: (a) for the Santa Cruz [left], (b) the Takatori [middle], and (c) Yarimca excitations [right].

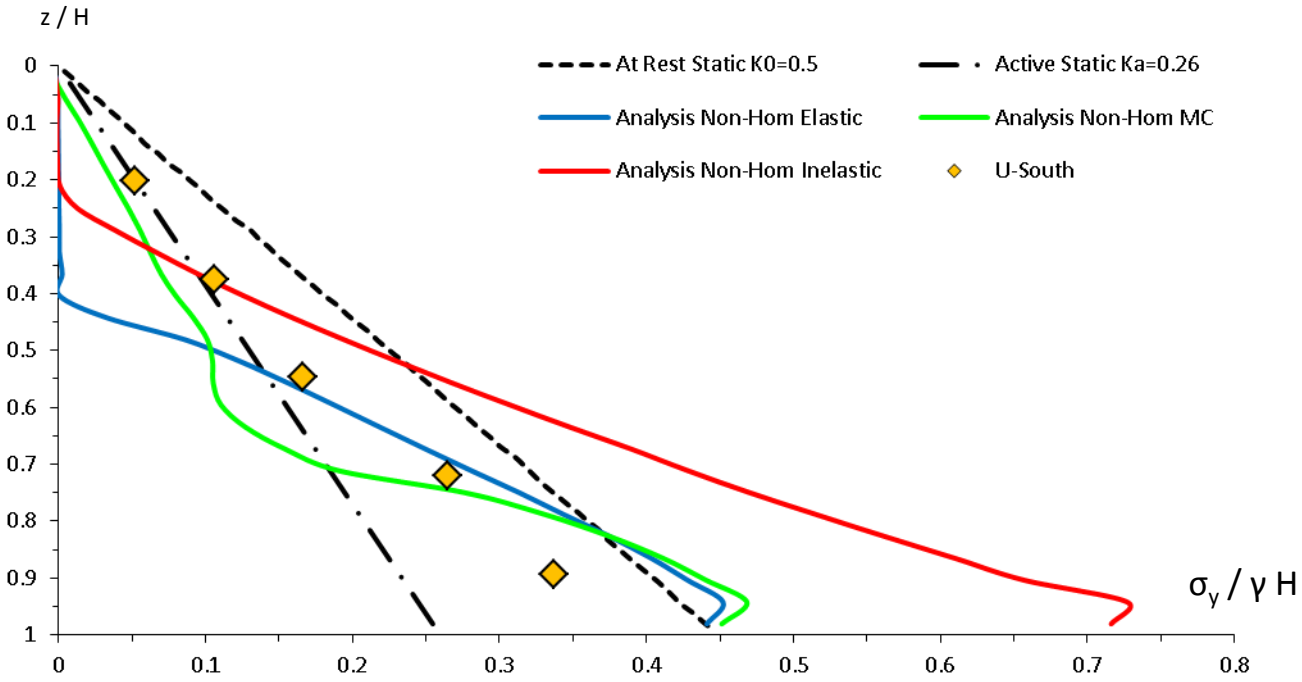

Figure 9. Normalized depth of the wall versus normalized static normal soil pressure [Excitation: Santa Cruz].

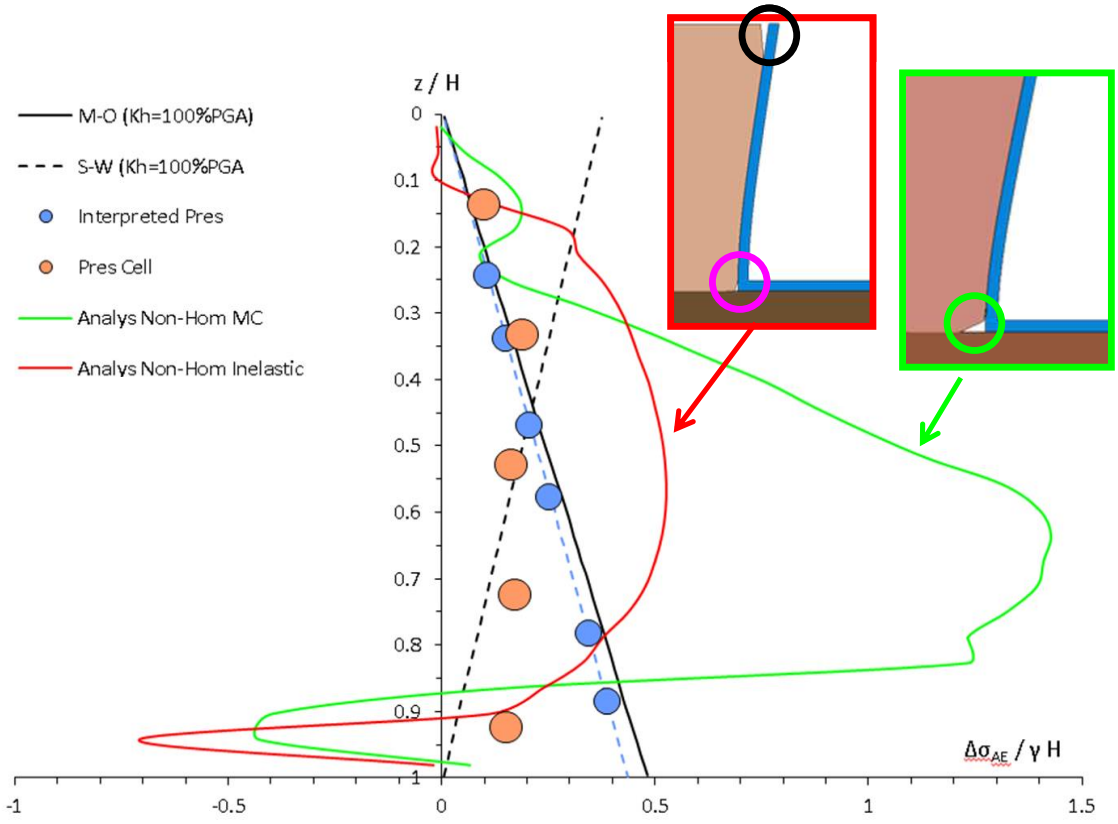

Figure 10. Normalized depth of the wall versus normalized dynamic normal soil pressure. [Excitation: Santa Cruz]

However, not all of our results were in such good agreement with the experimental ones. A discrepancy is noticed in the normalized static normal soil pressures σ_y / γ H, and an example can be seen in Figure 9. Notice that experimental response of the south (left) wall, with the yellow diamonds, is heading from the active static soil pressures in the upper side of the wall to the at rest static soil pressures in the lower side of the wall, a fact difficult to interpret with our inelastic analysis. For the soil pressures the response of our finite element model of the same non-homogeneous soil was tested with an elastic soil model and a Mohr-Coulomb (MC) soil model. The analysis with the MC soil model shows better results than both the inelastic soil model (modified Von Mises) and the elastic soil model.

The dynamic earth pressure distributions are presented in Figure 10, where the theoretical pressure distributions using the Mononobe-Okabe (M-O) and Seed and Whitman (SW) methods were all computed assuming k_h = 100%PGA. Observe that the true experimental response, with the light orange circles, shows a similar trend to the trend of dynamic pressures taken from the analysis of the inelastic soil model, whereas the interpreted dynamic pressure distribution is very close to the pseudo-static approach of the M-O method. It should be also pointed out that at the instant of the maximum moment the wall and the soil are moving together in an active phase condition.

It has to be mentioned, that in the experiment, soil pressures, p, were recorded by earth pressure sensors and were filtered using a low-pass Butterworth filter to reduce noise. In the experiment report by Mikola & Sitar it is stated that the pressure transducers, employed to measure p, have a manufacturer stated frequency response up to 100 Hz, which is sufficient for static earth Pressures, but they have difficulties to capture dynamic earth pressures, because centrifuge scaling requires a sensor with at least 500-700 Hz frequency sensitivity to fully record dynamic earth pressures. That is the reason why dynamic earth pressures were interpreted from the load cells as well as strain gage measurements. Maybe this is a reason of the experimental versus numerical soil pressures difference.

It is important to note, that all of the data represent the earth pressures and earth pressure distributions at the point of maximum dynamic moment, which does not necessarily correspond to the maximum observed earth pressure, as it is also noted by Mikola and Sitar (2013).

5. CONCLUSIONS

The paper verified numerically the seismic response of a U-shaped cantilever retaining wall comparing them with

experimental centrifuge results conducted by Mikola and Sitar (2013). 2-D analyses were conducted and the response of the retaining wall was investigated for the Takatori, Yarimca and Santa Cruz ground motions. Agreement was obtained for detailed acceleration time histories at characteristic points of the wall and the backfill soil and for bending moment distribution. Yet, the soil pressure distributions presented differences between the analysis and the experiment, mainly due to the pressure transducers frequency limitation (this experimental shortcoming has been noted in the report of Mikola and Sitar, 2013).

6. REFERENCES

[1] Al Atik, L. and Sitar, N. 2010. Seismic Earth Pressures on Cantilever Retaining Structures, *Journal of Geotechnical and Geoenvironmental Engineering*, ASCE, 136(10): 1324-1333.

[2] Al-Homoud, A.S. and Whitman, R.V. 1999. Seismic Analysis and Design of Rigid Bridge Abutments Considering Rotation and Sliding Incorporating Non-Linear Soil Behaviour, *Soil Dynamics and Earthquake Engineering*, Elsevier B. V., 18: 247-277.

[3] Anastasopoulos, I. Gelagoti, F. Kourkoulis, R. and Gazetas, G. 2011. Simplified constitutive model for simulation of cyclic response of shallow foundations: validation against laboratory tests, *Journal of Geotechnical and Geoenvironmental Engineering*, ASCE, 137(12): 1154-1168.

[4] Cai, Z. and Bathurst, R.J. 1995. Seismic response analysis of geosynthetic reinforced soil segmental retaining walls by finite element method, *Computers & Geotechnics*, Elsevier B.V., 17(4): 523-546.

[5] Cameron, W.I. and Green, R.A. 2004. Development of engineering procedure for evaluating lateral earth pressures for seismic design of cantilever retaining walls, *5th International PhD Symposium in Civil Engineering*, Balkema Publishers, Delft, The Netherlands, 2: 897-904.

[6] Dakoulas, P. and Gazetas, G. 2008. Insight into seismic earth and water pressures against caisson quay walls, *Géotechnique*, ICE Publishing, 58(2): 95–111.

[7] Garini, E. Gazetas, G. and Anastasopoulos, I. 2011. Asymmetric 'Newmark' Sliding Caused by Motions Containing Severe 'Directivity' and 'Fling' Pulses, *Géotechnique*, ICE Publishing, 61(9): 733-756.

[8] Garini, E. Tsantilas, L. and Gazetas, G. 2016. Seismic Response of Cantilever Retaining Walls: Verification of Centrifuge Experiments, *ICONHIC*, Chania, Greece, Conference Proceedings 207.

[9] Gazetas, G. Garini, E. Anastasopoulos, I. and Georgarakos, T. 2009. Effects of Near-Fault Ground Shaking on Sliding Systems, *J. Geotech. Geoenv. Engrg.*, ASCE, 135(12): 1906–1921.

[10] Gazetas, G. Psarropoulos, P.N. Anastasopoulos, I. and Gerolymos, N. 2004. Seismic behavior of flexible retaining systems subjected to short-duration moderately strong excitation. *Soil Dynamics and Earthquake Engineering*, Elsevier B. V., 24(7): 537-550.

[11] Gerolymos, N. and Gazetas, G. 2006. Static and Dynamic Response of Massive Caisson Foundations with Soil and Interface Nonlinearities-Validation and Results, *Soil Dynamics & Earthquake Engineering*, Elsevier B. V., 26(5): 377-394.

[12] Green, R.A. and Ebeling, R.M. 2002. Seismic analysis of cantilever retaining walls, Phase I, *Earthquake Engineering Research Program*, U.S. Army Corps of Engineers, Washington, DC, USA.

[13] Huang, C.C. 2005. Seismic Displacement of Soil Retaining Walls Situated on Slope, *J. Geotech. Geoenv. Engrg.*, ASCE, 31(9): 1108–1117.

[14] Madabhushi, S.P.G. and Zeng, X. 2007. Simulating Seismic Response of Cantilever Retaining Walls, *Journal of Geotechnical and Geoenvironmental Engineering*, ASCE, 133(5): 539-549.

[15] Mikola, G.R. and Sitar, N. 2013. Seismic Earth Pressures on Retaining Structures in Cohesionless Soils, *Report No. UCB GT 13-01*, Geotechnical Engineering, Dep. of Civil and Environ. Engineering, Univ. of California, Berkeley.

[16] Mononobe, N. and Matsuo, M. 1929. On the Determination of Earth Pressures during Earthquakes, Proceedings: *World Engineering Congress*, Tokyo, 9:177-185.

[17] Nadim, F. and Whitman, R.V. 1983. Coupled Sliding and Tilting of Gravity Retaining Walls, *J. Geot. Eng. Divis.*, ASCE, 109(7): 915–931.

[18] Nakamura, S. 2006. Re-Examination of Mononobe-Okabe Theory of Gravity Retaining Walls Using Centrifuge Model Tests, *Soils Found.*, ASCE, 46(2): 135-146.

[19] Okabe, S. 1924. General Theory on Earth Pressure and Seismic Stability of Retaining Wall and Dam, *J. Japan Society of Civil Engineers*, JSCE, 10(6): 1277-1323.

[20] Okabe, S. 1926. General Theory of Earth Pressures. *J. Japan Society of Civil Engineers*, JSCE, 12 (1): 123-134.

[21] Ortiz, L.A. Scott, R.F. and Lee, J. 1983. Dynamic Centrifuge Testing of a Cantilever Retaining Wall, *Earthq. Engng. Struct. Dyn.*, John Wiley & Sons Ltd, 11: 251–268.

[22] Psarropoulos, P.N. Klonaris, G. and Gazetas, G. 2005. Seismic Earth Pressures on Rigid and Flexible Retaining Walls, *Soil Dynamics and Earthquake Engineering*, Elsevier B. V., 25(7): 795-809.

[23] Richards, R. and Elms, D.G. 1979. Seismic behavior of gravity retaining walls. *J Geotech Eng Div*, ASCE,105:449–64.

[24] Seed, H.B. and Whitman, R.V. 1970. Design of Earth Retaining Structures for Dynamic Loads. *ASCE Specialty Conference on Lateral Stresses in the Ground and Design of Earth Retaining Structures*, Cornell Univ., Ithaca, N.Y., 1: 103-147.

[25] Theodorakopoulos, D.D. Chassiakos, A.P. and Beskos, D.E. 2001. Dynamic Pressures on Rigid Cantilever Walls Retaining Poroelastic Soil Media. Part I. First method of solution. *Soil Dynamics and Earthquake Engineering*, Elsevier B. V., 21: 315–338.

[26] Veletsos AS, Younan AH. 1994. Dynamic Modelling and Response of Soil-Wall Systems, *Journal of Geotechnical Engineering*, ASCE, 120 (12): 2155–2179.

[27] Wu, Y. and Prakash, S. 1999. Effect of Submergence on Seismic Displacement of Rigid Retaining Walls, Second International Conference on Earthquake Geotechnical Engineering, June 21-25, CD Rom, Lisboa, Portugal.

[28] Zeng, X. 1998. Seismic Response of Gravity Quay Walls. I: Cen-trifuge Modeling, *J. Geotech. Geoenv. Engrg.,* ASCE, 124(5): 406–417.